Numerical Heat Transfer, Part A, 40: 387–401, 2001

1040-7782/01 $12.00 + .00

HEAT AND MASS TRANSFER FROM A PERMEABLE CYLINDER IN A POROUS MEDIUM WITH MAGNETIC FIELD AND HEAT GENERATION/ABSORPTION EFFECTS

Ali J. Chamkha and Mir Mujtaba A. Quadri

Department of Mechanical and Industrial Engineering, Kuwait University, Safat, Kuwait

We formulate the problem of coupled heat and mass transfer by natural convection from a horizontal cylinder embedded in a uniform porous medium in the presence of an external magnetic field and internal heat generation or absorption effects. The cylinder surface is maintained at a constant temperature and a constant concentration and is permeable to allow for possible fluid wall suction or blowing. The resulting governing equations are nondimensionalized and transformed into a nonsimilar form and then solved numerically by an implicit, iterative, finite-difference method. Comparisons with previously published work are performed and excellent agreement is obtained. A parametric study of the physical parameters is conducted and a representative set of numerical results for the stream function, temperature, concentration profiles, and the Nusselt and Sherwood numbers is illustrated graphically to show interesting features of the solutions.

Coupled heat and mass transfer in fluid-saturated porous media finds applications in a variety of engineering processes such as heat exchanger devices, insulation systems, petroleum reservoirs, chemical catalytic reactors and processes, nuclear waste repositories, and others. There has been considerable work done on the study of flow and heat transfer in geometries with and without porous media (for instance, Nield and Bejan [1] and Churchill and Chu [2]).

The linear Darcy law, which accounts for the viscous effects and is applied for slow flow in porous media, was employed extensively in early works on porous media. For example, the problem of natural convection in a porous medium supported by an isothermal vertical plate was solved some time ago by Cheng and Minkowycz [3] using the Darcy law. It is well established now that the Darcy law is inadequate for modeling high velocity flow situations for which the pressure drop is a quadratic function of the flow rate. The deviation from the linear Darcy law is because of the porous medium inertial effects. Johnson and Cheng [4], Vafai and Tien [5], and Plumb and Huenefeld [6] were among the first to consider inertia effects in porous media.

Received 16 October 2000; accepted 24 February 2001.

Address correspondence to A. J. Chamkha, Department of Mechanical Engineering, P.O. Box 5969, Kuwait University, Safat 13060 Kuwait.

NOMENCLATURE

a	radius of the horizontal cylinder	T	temperature
B_o	magnetic induction	u	velocity in the x-direction
c	concentration	v	velocity in the y-direction
C	dimensionless concentration	v_w	suction or injection velocity
C^*	porous medium inertia coefficient	x	streamwise coordinate
D	mass diffusivity	y	transverse coordinate
f	dimensionless stream function	α_e	effective porous medium thermal diffusivity
f_w	transpiration or suction/injection parameter, $-v_w a/(\alpha_e \mathrm{Ra}^{1/2})$	β_c	coefficient of concentration expansion
F_r	dimensionless porous medium inertia parameter, $C^* K \alpha_e \mathrm{Ra}/(\nu a)$	β_T	coefficient of thermal expansion
g	gravitational acceleration	η	pseudosimilarity variable
h	heat transfer coefficient	θ	dimensionless temperature, $(T - T_\infty)/(T_w - T_\infty)$
h_m	mass transfer coefficient	ν	kinematic viscosity
K	porous medium permeability	σ	electrical conductivity
k_e	effective porous medium thermal conductivity	ξ	dimensionless coordinate
Le	Lewis number, α_e/D	ψ	stream function
M	Hartmann number, $(\sigma B_0^2 K/(\rho\nu))^{1/2}$	ϕ	dimensionless heat generation or absorption coefficient, $Q_o a^2/(\rho c_p \alpha_e \mathrm{Ra})$
N	buoyancy ratio, $\beta_c(c_w - c_\infty)/[\beta_T(T_w - T_\infty)]$	Φ	angle of the y-axis with respect to the vertical, x/a
Nu	Nusselt Number, ha/k_e		
Q_0	heat generation or absorption coefficient		
Ra	modified Rayleigh number, $g\beta_T K(T_w - T_\infty)a/(\nu\alpha_e)$	**Subscripts**	
Sh	Sherwood Number, $h_m a/D$	w	condition at the wall
		∞	condition at free stream

The problem of thermally driven natural convection flow about a horizontal cylinder embedded in a porous medium has been the subject of many investigations. For example, Merkin [7] has obtained a similarity solution, Fand et al. [8] have reported experimental results, and Nakayama and Koyama [9] have solved the problem using the integral method. Also, Ingham and Pop [10] and Pop et al. [11] have reported numerical results based on the finite-difference methodology. Aldoss and Ali [12] have recently considered mixed convection from a horizontal cylinder with suction and blowing in the presence of a magnetic field.

Recently, a significant number of investigations have been carried out on the effects of electrically conducting fluids such as liquid metals, water mixed with a little acid, and others in the presence of a magnetic field on the flow and heat transfer aspects (for example, Sparrow and Cess [13], Gray [14], Michiyoshi, et al. [15], Fumizawa [16], and Riley [17]). Also, the study of heat generation or absorption effects in moving fluids is important in view of several physical problems, such as fluids undergoing exothermic or endothermic chemical reactions (see Vajravelu and Hadjinicolaou [18] and Vajravelu and Nayfeh [19]). In addition, Kou and Lu [20] showed that the design of placing many electronic circuits into one small chip and more chips into a package results in high volumetric heat generation in the electronic equipment. This led to the consideration of heat generation effects in porous media. In addition, recently, Chamkha [21] analyzed the problem of non-Darcy free convection flow about a wedge and a cone embedded in a porous media in the presence of heat generation effects.

The coupled heat and mass transfer problem received relatively little attention. Trevisan and Bejan [22] considered combined heat and mass transfer by natural convection in a porous medium for various geometries. Bejan and Khair [23] reported on the natural convection boundary-layer flow in a saturated porous medium with combined heat and mass transfer. The coupled heat and mass buoyancy-induced inclined boundary layer in a porous medium was studied by Jang and Chang [24]. Later, Lai and Kulacki [25] extended the problem of Bejan and Khair [23] to include wall fluid injection effects. Yucel [26] has considered coupled heat and mass transfer about a vertical cylinder in porous media. Lai and Kulacki [27] have investigated coupled heat and mass transfer by natural convection from a sphere embedded in porous media. Recently Yih [28] has considered coupled heat and mass transfer by natural convection adjacent to a permeable horizontal cylinder in a saturated porous medium.

The purpose of this work is to extend the work of Yih [28] by including such effects as porous medium inertia, magnetic field, and heat generation or absorption effects.

GOVERNING EQUATIONS

Consider coupled heat and mass transfer by hydromagnetic natural convection from a horizontal permeable cylinder embedded in a uniform porous medium in the presence of heat generation or absorption effects. A uniform magnetic field is applied in the direction normal to the surface. The surface of the cylinder is maintained at a uniform temperature T_w and a uniform concentration c_w. Far from the wall, the free stream is kept at a constant temperature T_∞ and a constant concentration c_∞. Constant fluid suction or injection is imposed at the surface of the cylinder. The flow model and physical coordinate system is shown in Figure 1. The fluid is assumed to be Newtonian, viscous, and electrically conducting. The surface of the cylinder and the porous medium are assumed to be electrically insulating and are in local thermal equilibrium. All fluid properties are assumed constant except the density in the buoyancy term of the x-momentum equation. The magnetic Reynolds number is assumed small so that the induced magnetic field is neglected. In addition, no electric field is assumed to exist and the Hall effect is negligible. In the absence of an electric field, the small magnetic Reynolds number assumption uncouples Maxwell's equations from the Navier–Stokes equations (Cramer and Pai [29]). Taking all of the above assumptions into consideration and invoking the boundary-layer and Boussinesq approximations, we can write the governing equations based on the modified Darcy law, which includes the porous medium inertia effects, as (see Yih [28])

$$\frac{\partial u}{\partial x} + \frac{\partial v}{\partial y} = 0 \tag{1}$$

$$\left(1 + \frac{\sigma B_o^2 K}{\rho \nu} + \frac{2C^* K}{\nu} u\right) \frac{\partial u}{\partial y} = \frac{Kg}{\nu} \sin \Phi \left[\beta_T \frac{\partial T}{\partial y} + \beta_c \frac{\partial c}{\partial y}\right] \tag{2}$$

$$u \frac{\partial T}{\partial x} + v \frac{\partial T}{\partial y} = \alpha_e \frac{\partial^2 T}{\partial y^2} + \frac{Q_0}{\rho c_p} (T - T_\infty) \tag{3}$$

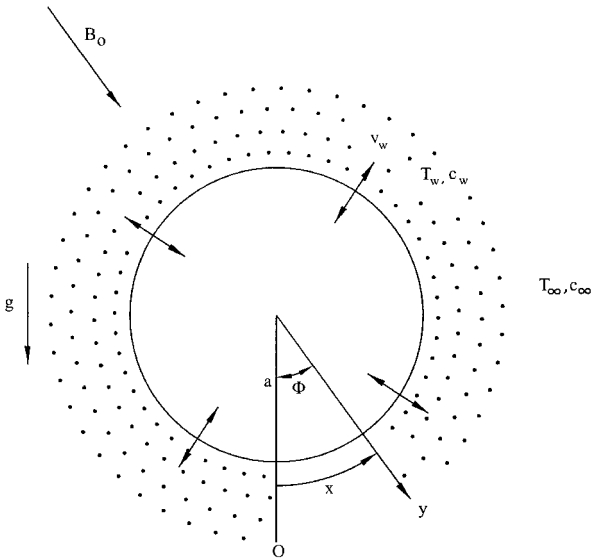

Figure 1. Flow model and physical coordinate system.

$$u\frac{\partial c}{\partial x}+v\frac{\partial c}{\partial y}=D\frac{\partial^2 c}{\partial y^2} \tag{4}$$

where x and y are the circumferential or streamwise and the transverse distances, respectively. u, v, T, and c are the fluid x-component of velocity, y-component of velocity, temperature, and concentration, respectively. ρ, ν, c_p, β_T, and β_c are the fluid density, kinematic viscosity, specific heat at constant pressure, coefficient of thermal expansion, and coefficient of concentration of expansion, respectively. K, C^* and α_e are the porous medium permeability, inertia coefficient, and effective thermal diffisuvity, respectively. σ, B_0, Q_0 and D are the electrical conductivity, magnetic induction, heat generation (>0) or absorption (<0) coefficient, and mass diffusivity, respectively. g and $\Phi = x/a$ (a being the radius of the cylinder) are the acceleration because of gravity and the angle of the y-axis with respect to the vertical ($0 \le \Phi \le \pi$).

The boundary conditions for this problem are given by

$$\begin{aligned} &y=0: && v=v_w \quad T=T_w \quad c=c_w \\ &y\to\infty: && u=0 \quad T=T_\infty \quad c=c_\infty \end{aligned} \tag{5}$$

where v_w is the suction (<0) or injection (>0) velocity.

It is convenient to transform Eqs. (1) through (5) by using the following nonsimilarity transformations reported earlier by Pop et al. [11] and Yih [28]:

$$\xi=\frac{x}{a} \quad \eta=\frac{y}{a}\mathrm{Ra}^{1/2} \quad \psi=\alpha_e\xi\mathrm{Ra}^{1/2}f(\xi,\eta)$$

$$\theta(\xi,n)=\frac{T-T_\infty}{T_w-T_\infty} \qquad C(\xi,n)=\frac{c-c_\infty}{c_w-c_\infty} \tag{6}$$

where $\mathrm{Ra} = g\beta_T K(T_W - T_\infty)a/\nu\alpha_e$ is the modified Rayleigh number and ψ is the dimensional stream function defined by the usual way as $u = \partial\psi/\partial y$ and $v = -\partial\psi/\partial x$. In terms of the above variables,

$$u = \frac{\alpha_e \xi \mathrm{Ra}}{a} f' \qquad v = -\frac{\alpha_e \mathrm{Ra}^{1/2}}{a}\left(f + \xi\frac{\partial f}{\partial \xi}\right) \tag{7}$$

Substituting Eqs. (6) into (1) through (5) yields the following nonsimilar equations and boundary conditions:

$$(1 + M^2 + 2\xi F_r f')f'' = \frac{\sin\xi}{\xi}(\theta' + NC') \tag{8}$$

$$\theta'' + f\theta' + \phi\theta + \xi\left(f'\frac{\partial\theta}{\partial\xi} - \theta'\frac{\partial f}{\partial\xi}\right) \tag{9}$$

$$\frac{1}{\mathrm{Le}}C'' + fC' = \xi\left(f'\frac{\partial C}{\partial\xi} - C'\frac{\partial f}{\partial\xi}\right) \tag{10}$$

$$\begin{aligned} &\eta = 0: \quad f = f_w \quad \theta = 1 \quad C = 1 \\ &\eta \to \infty: \quad f' = 0 \quad \theta = 0 \quad C = 0 \end{aligned} \tag{11}$$

where

$$\begin{aligned} &M^2 = \frac{\sigma B_o^2 K}{\rho\nu} \quad F_r = \frac{C^* K \alpha_e \mathrm{Ra}}{\nu a} \quad N = \frac{\beta_c(c_w - c_\infty)}{\beta_T(T_w - T_\infty)} \\ &\mathrm{Le} = \frac{\alpha_e}{D} \qquad \phi = \frac{Q_0 a^2}{\rho c_p \alpha_e \mathrm{Ra}} \qquad f_w = \frac{vw^a}{\alpha_e \mathrm{Ra}^{1/2}} \end{aligned} \tag{12}$$

are the square of the Hartmann number, dimensionless porous medium inertia coefficient, buoyancy ratio, Lewis number, dimensionless heat generation or absorption coefficient, and dimensionless suction ($f_w > 0$) or injection ($f_w < 0$) velocity.

The Nusselt and Sherwood numbers can be computed from the following relations:

$$\mathrm{Nu} = \frac{ha}{k_e} = -\mathrm{Ra}^{1/2}\theta'(\xi, \theta) \tag{13a}$$

$$\mathrm{Sh} = \frac{h_m a}{D} = -\mathrm{Ra}^{1/2} C(\xi, \theta) \tag{13b}$$

where h and h_m are the heat and mass transfer coefficients, respectively. k_e is the effective porous medium thermal conductivity.

NUMERICAL METHOD

The nonsimilar equations (8) through (10) are linearized and then descritized using three-point central difference quotients with variable step sizes in the

η-direction and using two-point backward difference formulae in the ξ-direction with a constant step size. The resulting equations are from a tridiagonal system of algebraic equations that can be solved by the well-known Thomas algorithm (see Blottmer [30]). The solution process starts at $\xi = 0$ and then marches forward using the solution at the previous line of constant ξ until it reaches $\xi = \pi$. Because of the nonlinearities of the equations, an iterative solution with successive over- or under-relaxation techniques is required. The convergence criterion required that the maximum absolute error between two successive iterations be 10^{-6}. The computational domain was made of 215 grids in the η-direction and 315 grids in the ξ-direction. A starting step size of 0.001 in the η-direction with an increase of 1.03 times the previous step size and a constant step size in the ξ-direction of 0.1 were found to give accurate results. The maximum value of η, which represented the ambient conditions, was assumed to be 50. The step sizes employed were arrived at after performing many numerical experimentations to assess grid independence. The accuracy of the aforementioned numerical method was validated by direct comparisons with the numerical results reported earlier by Merkin [7], Pop et al. [11], Bejan and Khair [23], and Yih [28] in the absence of magnetic field, heat generation, or absorption effects. Tables 1 and 2 present the results of these comparisons. It can be seen from these tables that excellent agreement between the results exists. These favorable comparisons lend confidence in the numerical results to be reported in the next section.

RESULTS AND DISCUSSION

Figures 2 through 4 display typical profiles for the dimensionless stream function, temperature, and concentration at the circumferential position $\xi = 0.5$ for various values of the Hartmann number, M and two values of the Lewis number Le,

Table 1. Values of $-\theta'(\xi, 0)$ for uniform wall temperature with $f_w = 0$, $F_r = 0$, $M = 0$, $N = 0$, and $\phi = 0$

ξ	Merkin [7]	Pop et al. [11]	Yih [28]	Present results
0.0	0.6276	0.6272	0.6276	0.6277
0.2	0.6245	0.6295	0.6245	0.6248
0.4	0.6151	0.6202	0.6151	0.6150
0.6	0.5996	0.6048	0.5996	0.6000
0.8	0.5781	0.5834	0.5781	0.5783
1.0	0.5508	0.5562	0.5508	0.5509
1.2	0.5180	0.5236	0.5180	0.5181
1.4	0.4800	0.4859	0.4800	0.4800
1.6	0.4373	0.4433	0.4371	0.4374
1.8	0.3901	0.3964	0.3899	0.3902
2.0	0.3391	0.3456	0.3387	0.3385
2.2	0.2847	0.2913	0.2843	0.2840
2.4	0.2274	0.2339	0.2271	0.2263
2.6	0.1679	0.1741	0.1677	0.1654
2.8	0.1067	0.1119	0.1066	0.1063
3.0	0.0444	0.0477	0.0446	0.0442
π	0.0000	0.0005	0.0001	0.0001

Table 2. Values of $-\theta'(0,0)/\sqrt{2}$ and $-C'(0,0)/\sqrt{2}$ for various values of N and Le with $f_w = 0$, $F_r = 0$, $M = 0$, and $\phi = 0$

		$-\theta'(0,0)/\sqrt{2}$			$-C'(0,0)/\sqrt{2}$		
N	Le	Bejan and Khair [23]	Yih [28]	Present results	Bejan and Khair [23]	Yih [28]	Present results
4	1	0.992	0.9922	0.9933	0.992	0.9922	0.9933
4	10	0.681	0.6810	0.6814	3.290	3.2897	3.2916
4	100	0.521	0.5208	0.5212	10.521	10.5201	10.5289
1	1	0.628	0.6276	0.6276	0.628	0.6276	0.6276
1	10	0.521	0.5214	0.5215	2.202	2.2021	2.2032
1	100	0.470	0.4700	0.4702	7.139	7.1388	7.1421
0	1	0.444	0.4439	0.4439	0.444	0.4439	0.4439
0	10	0.444	0.4439	0.4439	1.680	1.6802	1.6812
0	100	0.444	0.4439	0.4439	5.544	5.5444	5.5478

respectively. Imposition of a magnetic field to an electrically conducting fluid creates a draglike force called the Lorentz force. This force has the tendency to slow down the flow around the cylinder at the expense of increasing its temperature and concentration. This is depicted by the decreases in the stream function values and increases in the temperature and concentration values as M increases as shown in Figures 2 through 4. In addition, the increases in the temperature and concentration values as M increases are accompanied by increases in both the thermal and concentration boundary layers. Furthermore, for the value of buoyancy ratio $N = 1.0$

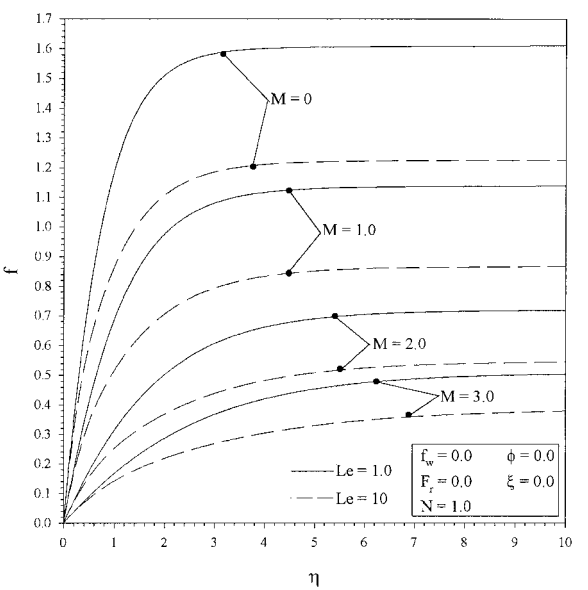

Figure 2. Effects of M and Le on stream function profiles.

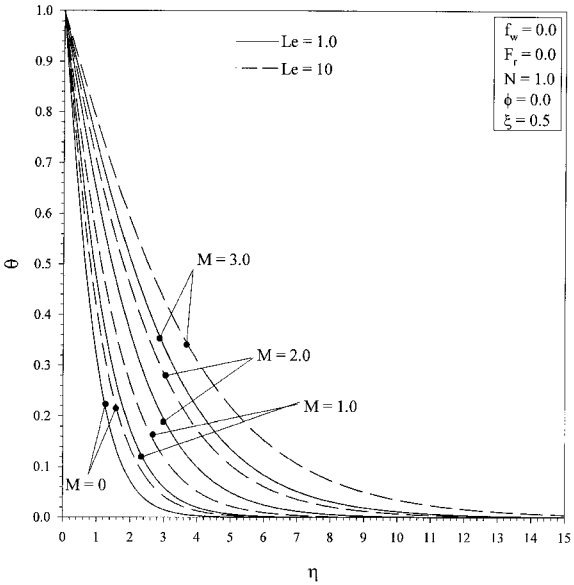

Figure 3. Effects of M and Le on temperature profiles.

(aiding flow), increases in the values of Le are seen to cause deceleration of the flow represented by decreases in the value of the stream function because of the reduction in the concentration buoyancy effect. Also, it is observed that while the concentration profile and its boundary layer decreases as Le increases, the temperature profile

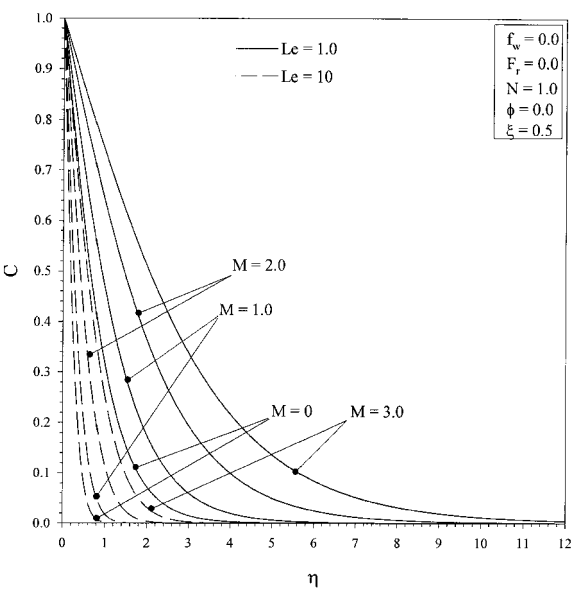

Figure 4. Effects of M and Le on concentration profiles.

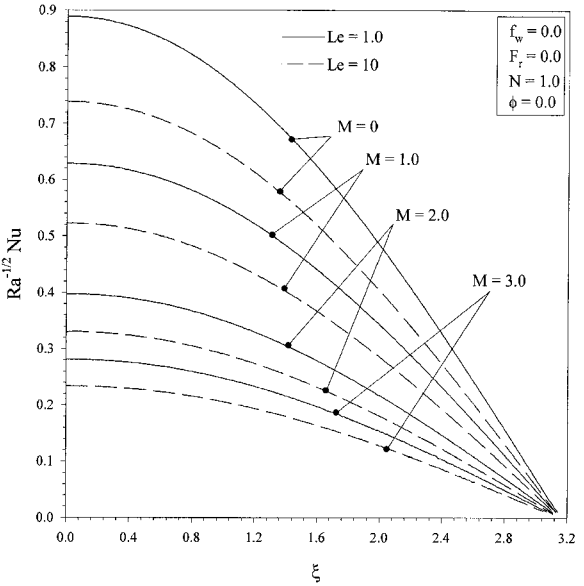

Figure 5. Effects of M and Le on Nusselt number.

and its boundary layer increases as Le increases. These behaviors are obvious from Figures 2 through 4.

Figures 5 and 6 illustrate the behaviors of the distributions of the Nusselt and Sherwood numbers because of changes in the values of M and Le, respectively. For a

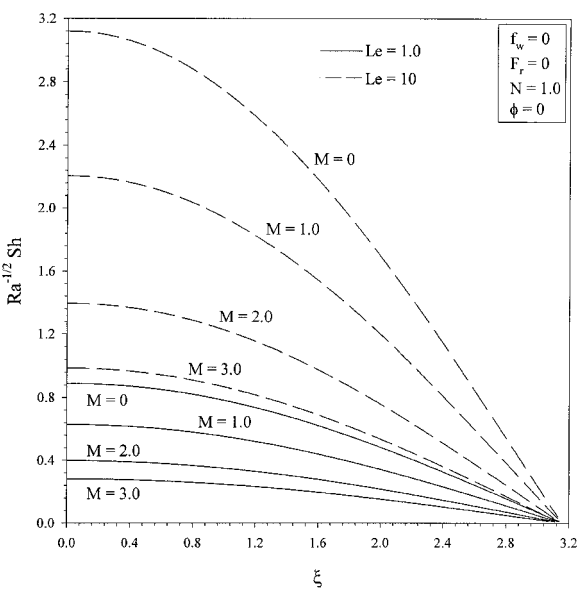

Figure 6. Effects of M and Le on Sherwood number.

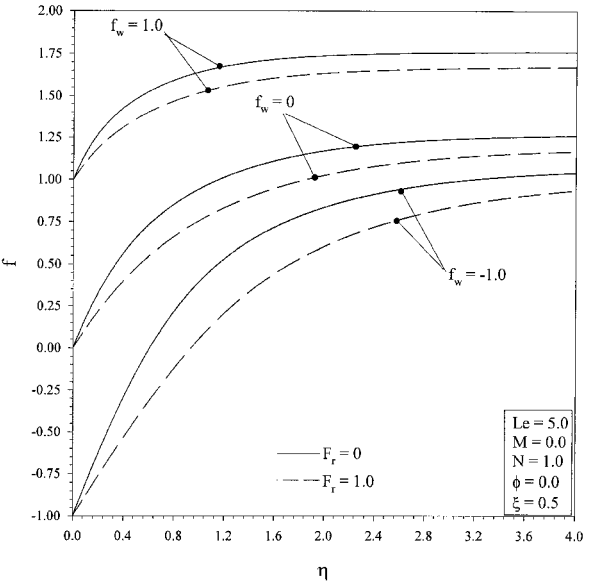

Figure 7. Effects of f_w and F_r on stream function profiles.

given Le, increasing the Hartmann number causes the negative slopes of the temperature and concentration profiles at the cylinder surface ($-\theta'(\xi,0)$ and $-C'(\xi,0)$) to decrease at every circumferential position ξ. This is clear from Figures 3 and 4. This behavior results in decreases in both the Nusselt and Sherwood numbers. Also,

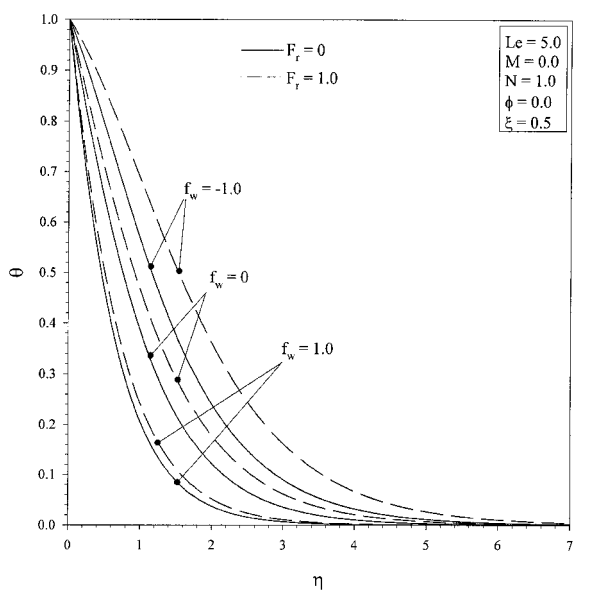

Figure 8. Effects of f_w and F_r on temperature profiles.

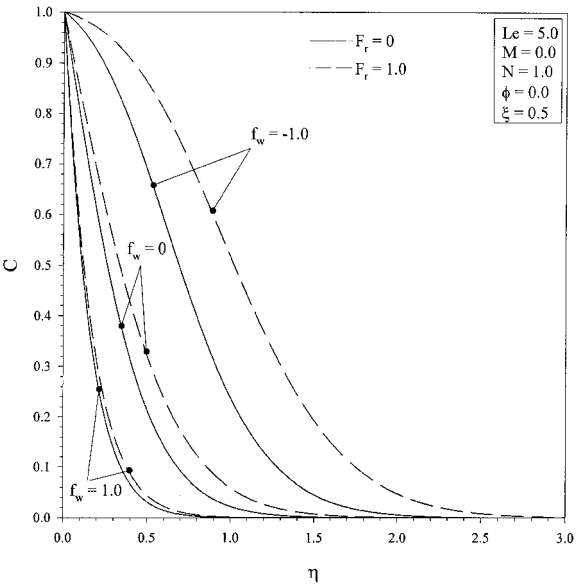

Figure 9. Effects of f_w and F_r on concentration profiles.

for the case of aiding flow ($N > 0$), increases in the values of Le produce decreases in the Nusselt number and increases in the Sherwood number. This is associated with the increases in the thermal boundary layer and decreases in the concentration boundary layer as Le increases as discussed earlier.

Figures 7 through 9 present the effects of the suction or injection parameter f_w and the porous medium inertia parameter F_r on the stream function, temperature, and concentration profiles at $\xi = 0.5$, respectively. Imposition of wall fluid suction ($f_w > 0$) tends to enhance the flow around the cylinder at the expense of reduced temperature and concentration profiles and their boundary layers. On the other hand, imposition of fluid injection or blowing at the cylinder surface ($f_w < 0$) produces the opposite behavior, namely, a decrease in the flow stream and increases in the temperature and concentration as depicted in Figures 7 through 9. Similar to the magnetic field, the effect of the porous medium inertia parameter F_r is predicted to decrease the stream function and to increase the temperature and concentration values. This is expected because the porous medium inertia effect produces a resistive effect on the flow similar to that of the magnetic field.

In Figures 10 and 11, the effects of f_w and F_r on the Nusselt and Sherwood numbers, respectively, are presented. In these figures, it is predicted that both the Nusselt and Sherwood numbers increase as the suction/injection parameter f_w increases. These behaviors are related to the decreases in both the thermal and concentration boundary layers as f_w increases. In general, the effect of F_r is seen to decrease both the Nusselt and Sherwood numbers except for the cases of $f_w \geq 0$ where the Nusselt number tends to increase beyond the circumferential position $\xi \approx 2.18$ for $f_w = 1.0$ and $\xi = 2.8$ for $f_w = 0$ while the Sherwood number increases beyond $\xi = 2.0$ for $f_w = 1.0$ and $\xi = 2.8$ for $f_w = 0$. This is associated with the third

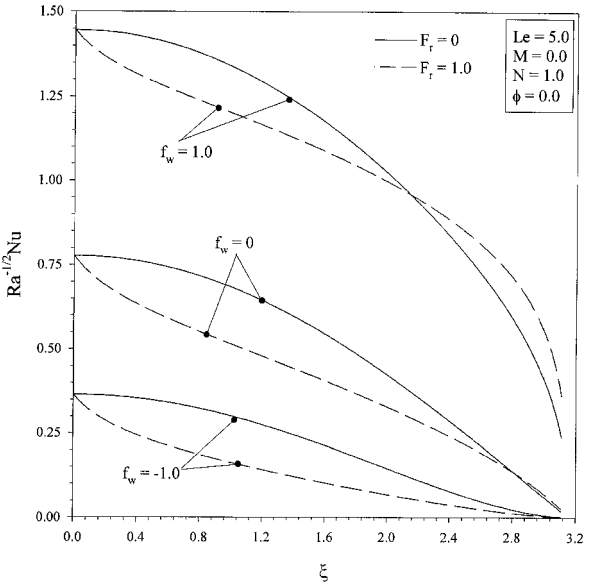

Figure 10. Effects of f_w and F_r on Nusselt number.

term of Eq. (8), which increases as ξ increases causing the thermal and concentration boundary layers to increase.

Figures 12 and 13 show the influence of the dimensionless heat generation or absorption coefficient ϕ on the Nusselt and Sherwood numbers for the two buoyancy

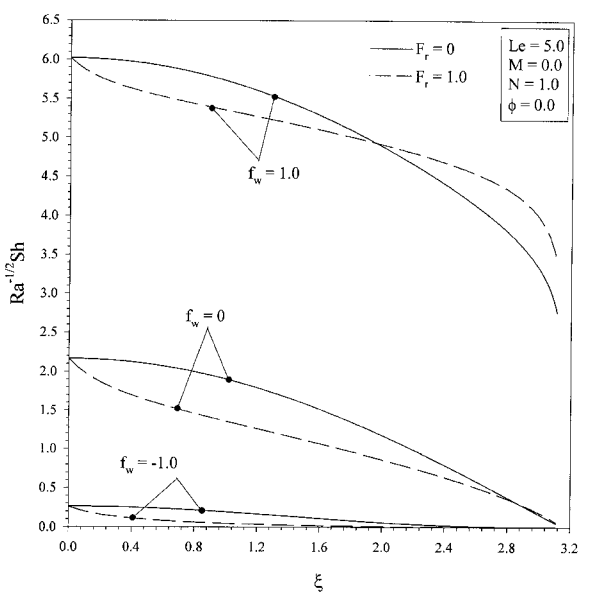

Figure 11. Effects of f_w and F_r on Sherwood number.

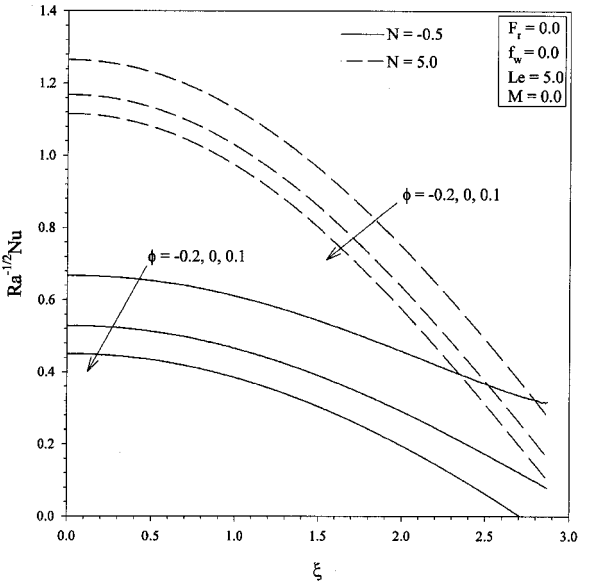

Figure 12. Effects of N and ϕ on Nusselt number.

ratio values $N = -0.5$ (buoyancy-opposing flow), and $N = 5.0$ (buoyancy-aiding flow), respectively. Increases in the heat generation/absorption coefficient ϕ have the tendency to increase the thermal boundary layer. This causes the Nusselt number to decrease at every circumferential position ξ as ϕ increases for both buoyancy-aiding and buoyancy-opposing flows. This is clear from Figure 12. However, increasing the

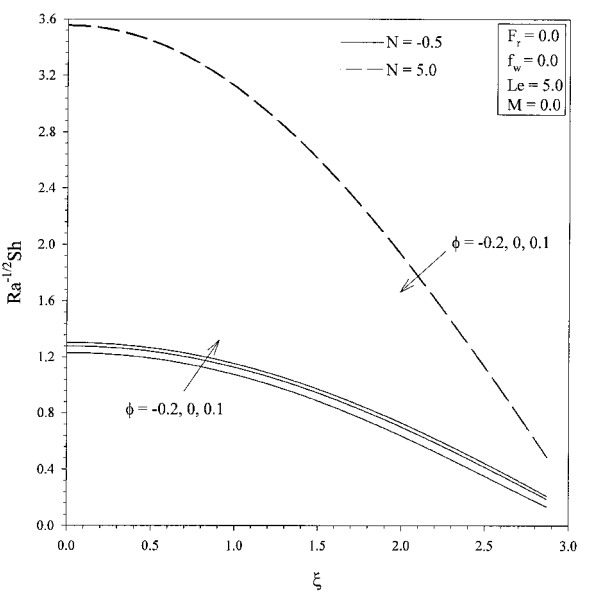

Figure 13. Effects of N and ϕ on Sherwood number.

value of ϕ has the tendency to decrease the Sherwood number for buoyancy-aiding flow ($N = 5.0$) while it causes the Sherwood number to increase for buoyancy-opposing flow ($N = -0.5$). These behaviors are shown in Figure 13. The effects of increasing the buoyancy ratio is predicted to increase both the Nusselt and Sherwood numbers.

CONCLUSION

This work considered coupled heat and mass transfer by natural convection from a permeable horizontal cylinder embedded in a uniform porous medium in the presence of porous medium inertia, magnetic field, and heat generation or absorption effects. The surface of the cylinder was maintained at constant temperature and concentration. The obtained transformed nonsimilar equations were solved numerically by an implicit, tridiagonal finite-difference method. The obtained results were checked against previously published work and were found to be in excellent agreement. Numerical results for the stream function, temperature, and concentration profiles as well as the Nusselt and Sherwood numbers were reported graphically. It was found that both the Nusselt and Sherwood numbers increased because of increases in either the suction/injection parameter or the buoyancy ratio. However, they decreased because of increases in either the Hartmann number or the porous medium inertia parameter. For the case of buoyancy-aiding flow, increases in the values of produced decreases in the Nusselt number and increases in the Sherwood number. Finally, for the buoyancy-aiding flow situation, the heat generation effects were found to decrease both the Nusselt and Sherwood numbers. It is hoped that the present work will be useful for validating more complex investigations dealing with heat and mass transfer from cylinders embedded in porous media.

REFERENCES

1. D. A. Nield and A. Bejan, *Convection in Porous Media*, 2nd ed., Springer-Verlag, New York, 1999.
2. S. W. Churchill and H. H. S. Chu, Correlating Equations for Laminar and Turbulent Free Convection from a Vertical Plate, *Int. J. Heat Mass Transfer*, vol. 18, pp. 323–1329, 1975.
3. P. Cheng and W. J. Minkowycz, Free Convection about a Vertical Flat Plate Embedded in a Porous Medium with Application to Heat Transfer from a Dike, *J. of Geophy*, vol. 82, pp. 2040–2044, 1977.
4. C. H. Johnson and P. Cheng, Possible Similarity Solutions for Free Convection Boundary-Layers Adjacent to Flat Plates in Porous Media, *Int. J. Heat Mass Transfer*, vol. 21, pp. 709–718, 1978.
5. K. Vafai and C. L. Tien, Boundary and Inertia Effects on Flow and Heat Transfer in Porous Media, *Int. J. Heat Mass Transfer*, vol. 24, pp. 195–203, 1981.
6. O. A. Plumb and T. C. Huenefeld, Non-Darcy Natural-Convection from Heated Surfaces in Saturated Porous Media, *Int. J. Heat Mass Transfer*, vol. 24, pp. 765–768, 1981.
7. J. H. Merkin, Free Convection Boundary Layers on Axisymmetric and Two-Dimensional Bodies of Arbitrary Shape in a Saturated Porous Medium, *Int. J. Heat Mass Transfer*, vol. 22, pp. 1461–1462, 1979.
8. R. M. Fand, T. E. Steinberger, and P. Cheng, Natural Convection Heat Transfer from a Horizontal Cylinder Embedded in a Porous Medium, *Int. J. Heat Mass Transfer*, vol. 29, pp. 119–133, 1986.

9. A. Nakayama and H. Koyama, Free Convection Heat Transfer over a Nonisothermal Body of Arbitrary Shape Embedded in a Fluid-Saturated Porous Medium, *ASME J. Heat Transfer*, vol. 109, pp. 125–130, 1987.
10. D. B. Ingham and I. Pop, Natural Convection about a Heated Horizontal Cylinder in a Porous Medium, *J. Fluid Mech.*, vol. 184, pp. 157–181, 1987.
11. I. Pop, M. Kumari, and G. Nath, Free Convection about Cylinders of Elliptic Cross Section Embedded in a Porous Medium, *Int. J. Engg. Sci.*, vol. 30, pp. 35–45, 1992.
12. T. K. Aldoss and Y. D. Ali, MHD Free Forced Convection from a Horizontal Cylinder with Suction and Blowing, *Int. Commun. Heat Mass Transfer*, vol. 24, pp. 683–693, 1997.
13. E. M. Sparrow and R. D. Cess, Effects of Magnetic Field on Free Convection Heat Transfer, *Int. J. Heat Mass Transfer*, vol. 3, pp. 267–274, 1961.
14. D. D. Gray, The Laminar Wall Plume in a Transverse Magnetic Field, *Int. J. Heat Mass Transfer*, vol. 22, pp. 1155–1158, 1979.
15. I. Michiyoshi, I. Takahashi, and A. Serizawa, Natural Convection Heat Transfer from a Horizontal Cylinder to Mercury under Magnetic Field, *Int. J. Heat Mass Transfer*, vol. 19, pp. 1021–1029, 1976.
16. M. Fumizawa, Natural Convection Experiment with Liquid NaK under Transverse Magnetic Field, *J. Nuclear Science and Technology*, vol. 17, pp. 10–17, 1980.
17. N. Riley, Magnetohydrodynamics Free Convection, *J. Fluid Mech.*, vol. 18, pp. 577–586, 1964.
18. K. Vajravelu and A. Hadjinicolaou, Heat Transfer in a Viscous Fluid over a Stretching Sheet with Viscous Dissipation and Internal Heat Generation, *Int. Commun. Heat Mass Transfer*, vol. 20, pp. 417–430, 1993.
19. K. Vajravelu and J. Nayfeh, Hydromagnetic Convection at a Cone and a Wedge, *Int. Commun. Heat Mass Transfer*, vol. 19, pp. 701–710, 1992.
20. H. S. Kou and K. T. Lu, Combined Boundary and Inertia Effects for Fully Developed Mixed Convection in a Vertical Channel Embedded in Porous Media, *Int. Commun. Heat Mass Transfer*, vol. 20, pp. 333–345, 1993.
21. A. J. Chamkha, Non-Darcy Hydromagnetic Free Convection from a Cone and a Wedge in Porous Media, *Int. Commun. Heat Mass Transfer*, vol. 23, pp. 875–887, 1996.
22. O. V. Trevisan and A. Bejan, Mass and Heat Transfer by Natural Convection in a Vertical Slot Filled with Porous Medium, *Int. J. Heat Mass Transfer*, vol. 29, pp. 403–415, 1990.
23. A. Bejan and K. R. Khair, Heat and Mass Transfer by Natural Convection in a Porous Medium, *Int. Commun. Heat Mass Transfer*, vol. 28, pp. 909–918, 1985.
24. J. Y. Jang and W. J. Chang, Buoyancy-Induced Inclined Boundary Layer Flow in a Porous Medium Resulting from Combined Heat and Mass Buoyancy Effects, *Int. Commun. Heat Mass Transfer*, vol. 15, pp. 17–30, 1988.
25. F. C. Lai and F. A. Kulacki, Non-Darcy Mixed Convection along a Vertical Wall in a Saturated Porous Medium, *Int. J. Heat Mass Transfer*, vol. 113, pp. 252–255, 1991.
26. A. Yucel, Natural Convection of Heat and Mass Transfer along a Vertical Cylinder in a Porous Medium, *Int. J. Heat Mass Transfer*, vol. 33, pp. 2265–2274, 1990.
27. F. C. Lai and F. A. Kulacki, Coupled Heat and Mass Transfer from a Sphere Buried in an Infinite Porous Medium, *Int. J. Heat Mass Transfer*, vol. 33, pp. 209–215, 1990.
28. K. A. Yih, Coupled Heat and Mass Transfer by Natural Convection Adjacent to a Permeable Horizontal Cylinder in a Saturated Porous Medium, *Int. Commun. Heat Mass Transfer*, vol. 26, pp. 431–440, 1999.
29. K. R. Cramer and S. I. Pai, *Magneto Fluid Dynamics for Engineers and Applied Physicists*, McGraw-Hill, New York, 1973.
30. F. G. Blottner, Finite-Difference Methods of Solution of the Boundary-Layer Equations, *AIAA Journal*, vol. 8, pp. 193–205, 1970.